Immune Expression and Inhibition of Heat Shock Protein 90 in Uveal Melanoma

Dana Faingold,[1] Jean-Claude Marshall,[1] Emilia Antecka,[1] Sebastian Di Cesare,[1] Alexandre N. Odashiro,[1] Silvin Bakalian,[1] Bruno F. Fernandes,[1] and Miguel N. Burnier, Jr.[1,2]

Abstract

Purpose: To examine the immunohistochemical profile of heat shock protein 90 (Hsp90) in uveal melanoma and the cytotoxicity of an Hsp90 inhibitor, 17-allylamino-17-demethoxygeldanamycin (17-AAG), in uveal melanoma cell lines.

Experimental Design: Hsp90 expression was determined by immunohistochemistry in 44 paraffin-embedded sections of primary human uveal melanoma and in five uveal melanoma cell lines (92.1, OCM-1, MKT-BR, SP6.5, and UW-1). Sulforhodamine B – based proliferation assay was used to compare uveal melanoma cell growth with a range of concentrations of 17-AAG. Changes in cell migration, invasion, cell cycle fractions, and apoptotic activity were also evaluated. Expression of intracellular proteins was determined by Western blot analysis after 17-AAG exposure.

Results: Immunohistochemical expression of Hsp90 was identified in 68% of the paraffin-embedded sections and significantly associated with largest tumor dimension ($P = 0.03$). 17-AAG significantly reduced the proliferation rates of uveal melanoma cell lines, with concentrations of 100 to 0.1 μmol/L. 17-AAG also significantly reduced the migratory and invasive capabilities of uveal melanoma cell lines. Cell cycle analysis showed that 17-AAG induced accumulations of cells in G_1. Caspase-3 protease activity analysis, a marker for apoptosis, showed a significant increase after drug exposure. The cytotoxic effect of 17-AAG was associated with decreased levels of phosphorylated Akt and cyclin-dependent kinase 4.

Conclusions: The immunohistochemical expression of Hsp90 in uveal melanoma indicates worse prognosis. To the best of our knowledge, this is the first report showing the inhibitory effect on uveal melanoma cells using 17-AAG to target Hsp90. Therefore, Hsp90 may be used as a potential target for treatment of patients with uveal melanoma.

Uveal melanoma is the most common primary intraocular malignancy in adults, with survival rates at 5, 10, and 15 years of 65%, 52%, and 46%, respectively (1). Metastatic disease disseminates predominantly to the liver in 71.4% to 87% of the patients and chemotherapy is minimally effective (2).

One promising target intensely researched in other malignancies is heat shock protein 90 (Hsp90; ref. 3). Hsp90 contributes to cell survival through protective mechanisms as protein folding, translocation between cellular compartments, and suppression of protein aggregation (4). Hsp90 is overexpressed in several malignancies (5) and interacts with several client proteins, including growth factor receptors, signaling kinases (Akt and Raf-1), and cell cycle regulators [cyclin-dependent kinase (CDK) 4], which regulate signal transduction, cell cycle control, and antiapoptotic mechanisms. The disruption of Hsp90 intrinsic ATPase activity results in degradation of the client proteins via the ubiquitin-proteasome pathway (6).

17-Allylamino-17-demethoxygeldanamycin (17-AAG) is a specific Hsp90 inhibitor, which yields similar results to Hsp90 small interfering RNA (7). 17-AAG has been shown to reduce malignant phenotype in several cancer cell lines and is now being investigated in multiple cancer trials (8, 9). The potential roles of Hsp90 in proliferation and progression of uveal melanoma have not been investigated to date. The purpose of this study was to characterize the expression of Hsp90 in uveal melanoma and to investigate the effects of 17-AAG administration to five frequently studied uveal melanoma cell lines (10).

Materials and Methods

Patients and tissue samples. Clinicopathologic data from 44 patients with uveal melanoma were collected from the archives of the Henry C. Witelson Ocular Pathology Laboratory, McGill University (Montreal, Quebec, Canada). Data included age, gender, previous ocular radiation

Authors' Affiliations: [1]Department of Ophthalmology and Pathology, The McGill University Health Center and Henry C. Witelson Ocular Pathology Laboratory, Montreal, Quebec, Canada and [2]Department of Ophthalmology, Federal University of São Paulo (UNIFESP/EPM), São Paulo, Brazil

Received 4/17/07; revised 10/26/07; accepted 11/5/07.

Grant support: Henry R. Shibata Fellowship, Cedars Cancer Institute (D. Faingold).

The costs of publication of this article were defrayed in part by the payment of page charges. This article must therefore be hereby marked *advertisement* in accordance with 18 U.S.C. Section 1734 solely to indicate this fact.

Requests for reprints: Dana Faingold, Department of Ophthalmology and Pathology, The McGill University Health Center and Henry C. Witelson Ocular Pathology Laboratory, 3775 University Street, Room 216, Montreal, Quebec, Canada H3A-2B4. Phone: 514-392-7192, ext. 00384; Fax: 514-398-5728; E-mail: faingolddana@yahoo.com.

doi:10.1158/1078-0432.CCR-07-0926

therapy, development of distant metastasis, and follow-up time. Patients were divided into two groups based on the treatment received: group one (primary enucleation; $n = 26$) and group two [patients treated with enucleation after previous ruthenium plaque radiotherapy ($n = 16$) or after transscleral thermotherapy ($n = 2$)]. Immunohistochemical expression was correlated with known prognostic factors, such as cell type (11) and largest tumor dimension (LTD; ref. 12). Tumors were classified as spindle when composed solely of spindle cells, epithelioid when composed only of epithelioid cells, and mixed when composed of any proportion of spindle and epithelioid cells. The follow-up time, measured in months, was defined as the time interval between the date of diagnosis of the primary tumor and the date of the detection of metastatic disease or last clinical consultation with clinical status.

All data accumulation was in accordance with Canada and Province of Quebec legislation and the tenets of the Declaration of Helsinki.

Immunohistochemistry. Formalin-fixed, paraffin-embedded sections of the specimens were H&E stained for histopathologic assessment by two ocular pathologists.

Immunohistochemistry was done using the Ventana benchmark machine according to the protocol (Ventana Medical Systems, Inc.). The fully automated processing of bar code–labeled slides included baking of the slides, solvent-free deparaffinization, and CC1 [Tris-EDTA buffer (pH 8.0)] antigen retrieval. Slides were incubated with the monoclonal mouse anti-Hsp90 (StressGen) at a dilution of 1:100 for 30 min at 37°C followed by application of biotinylated secondary antibody (8 min, 37°C) and then an avidin/streptavidin enzyme conjugate complex (8 min, 37°C).

Finally, the antibody was detected by Fast Red chromogenic substrate and counterstained with hematoxylin.

As a positive control, sections of skin melanoma were used (13), and for negative controls, the primary antibody was omitted.

Immunocytochemistry. Cytospins were prepared from the five uveal melanoma cell lines 92.1, OCM-1, MKT-BR, SP6.5, and UW.1 (200,000 cells per spin) using the Cytospin 3 centrifuge (Shandon, Inc.) and fixed with 2% paraformaldehyde for 20 min. The cytospins were stained according to the streptavidin-biotin complex/horseradish peroxidase protocol (DakoCytomation Denmark A/S) with monoclonal mouse anti-Hsp90 primary antibody.

Immunofluorescence analysis was done on adherent cell culture in chamber slides and immunostained for Hsp90 and Hsp90α (StressGen) using a FITC-conjugated secondary antibody (Sigma-Aldrich). Counterstaining was done using SYTO red fluorescent nucleic stain (Invitrogen) and visualized by confocal microscopy (Olympus confocal microscope).

Microscopic classification. Specimens were classified according to the percentage of positive staining and intensity based on a quick score method (14) for immunohistochemical semiquantitation and scored 1 when 0% to 25% of the tumor cells per section stained, scored 2 when 25% to 50% of tumor cells per section stained, and scored 3 when >50% of tumor cells per section stained. The staining intensity was scored as follows: 0 to 1, weak staining; 2, moderate staining; and 3, intense staining. The cases were divided between low Hsp90 expression scores (0–4) representing low intensity and <50% positive cells and high Hsp90 expression scores (5 and 6) representing moderate and intense staining and >50% positive cells. This division was based on previous results of quantitative analysis of immunohistochemistry of Hsp90 in urothelial carcinoma (15).

Cell culture. Four human uveal melanoma cell lines (92.1, SP6.5, MKT-BR, and OCM-1) and one human uveal transformed melanocyte cell line (UW-1) were incubated at 37°C in a humidified 5% CO_2-enriched atmosphere. The cells were cultured in RPMI 1640 (Invitrogen) supplemented with 5% heat-inactivated fetal bovine serum, 1% fungizone, and 1% penicillin-streptomycin. The cultures were grown to confluence and passaged by treatment with 0.05% trypsin in EDTA (Fisher) at 37°C and washed in 7 mL RPMI 1640 before being centrifuged at $120 \times g$ for 10 min to form a pellet. Cells were then suspended in 1 mL of medium and counted using the trypan blue dye exclusion test. The uveal melanoma cell lines 92.1, SP6.5, and MKT-BR were established by Dr. Jager (University Hospital Leiden, Leiden, the Netherlands; ref. 16), Dr. Pelletier (Laval University, Quebec, Quebec, Canada), and Dr. Belkhou (CJF Institut National de la Sante et de la Recherche Medicale, Paris, France), respectively. Dr. Albert (University of Wisconsin, Madison, WI) established the OCM-1 and UW-1 cell lines (17).

In vitro *proliferation assay.* The sulforhodamine B–based assay kit (TOX-6, Sigma-Aldrich) was done as per the National Cancer Institute protocol. Briefly, the uveal melanoma cell lines were seeded into wells at a concentration of 2.5×10^3 cells per well in a minimum of six wells per cell line. A row of eight wells exposed to only RPMI 1640 was used as a control. The 17-AAG drug (A.G. Scientific, Inc.) was reconstituted in serum-free RPMI 1640 (300 ng/mL). Cells with and without 17-AAG at different dilutions (100-0.001 μmol/L) were allowed to incubate for 48 h following cell seeding. Cells were fixed to the bottom of the wells using a solution of 50% trichloroacetic acid for 1 h at 4°C. Plates were then rinsed with distilled water, to remove trichloroacetic acid and medium, and air dried. The sulforhodamine B dye was added to each well, allowed to stain for 25 min, and subsequently removed by washing with a 10% acetic acid solution. The dye that was incorporated into the fixed cells at the bottom of the wells was solubilized in a 10 mmol/L solution of Tris. The absorbance of the solute was measured using a microplate reader at a wavelength of 510 nm.

Migration assay. A QCM 24-well colorimetric cell migration assay (Chemicon) was used for this experiment as per the manufacturer's recommendations. Briefly, uveal melanoma cell lines with and without 17-AAG (10 μmol/L) were trypsinized and seeded at a concentration of 1×10^6 cells/mL in serum-free RPMI 1640 and placed in the upper well insert of a QCM 24-well colorimetric cell migration assay. Cells (1.25×10^5) were added to the upper chamber in RPMI 1640 with 0.1% fetal bovine serum. CXCL8 was used as a chemoattractant (18) after being reconstituted and diluted to appropriate predetermined optimum concentrations in serum-free RPMI 1640 (CXCL8: 300 ng/mL). The experiments were done in triplicate for all five cell lines. The 24-well plates were then incubated for 24 h in a humidified 5% CO_2-enriched atmosphere. Cells that migrated through the 8-μm pore membranes, located at the bottom of every well insert, were stained and eluted. The absorbance of the stained cells was read by a colorimetric plate reader at 560 nm.

Invasion assay. A modified Boyden chamber consisting of polyethylene terephthalate membrane with 8-μm-diameter pores precoated with Matrigel, an artificial basement membrane (Becton Dickinson Labware), was used as previously described to assay for invasive ability (19). A polyethylene terephthalate membrane without Matrigel was used as a control.

Briefly, 1.25×10^5 cells with and without 10 μmol/L/mL 17-AAG were added to the upper chamber in RPMI 1640 with 0.1% fetal bovine serum. RPMI 1640 with 10% fetal bovine serum was added to the lower chamber as a chemoattractant to obtain the baseline invasive ability of the cell lines. The chambers were then incubated at 37°C in 5% CO_2-enriched atmosphere for 48 h to allow for cellular invasion through the Matrigel.

Noninvading cells were removed from the upper chamber by gently wiping the surface of the membrane with a moist cotton swab. Membranes were removed and then stained using a Diff-Quick staining set. Stained cells were counted microscopically in 20 high-powered (×400) fields. Only cells whose nuclei had completely invaded through the membrane were counted. Each experimental condition, including control, was done in triplicate and the average number of invading cells was then calculated for all experimental conditions.

Percentage invasion was determined for each cell line under each experimental condition using the following formula: % invasion = (mean number of cells invading through the Matrigel/mean number of cells migrating through control polyethylene terephthalate membrane) multiplied by a hundred.

Cell cycle analysis. Cells were passaged and then counted using the trypan blue dye exclusion test as previously described. Untreated uveal

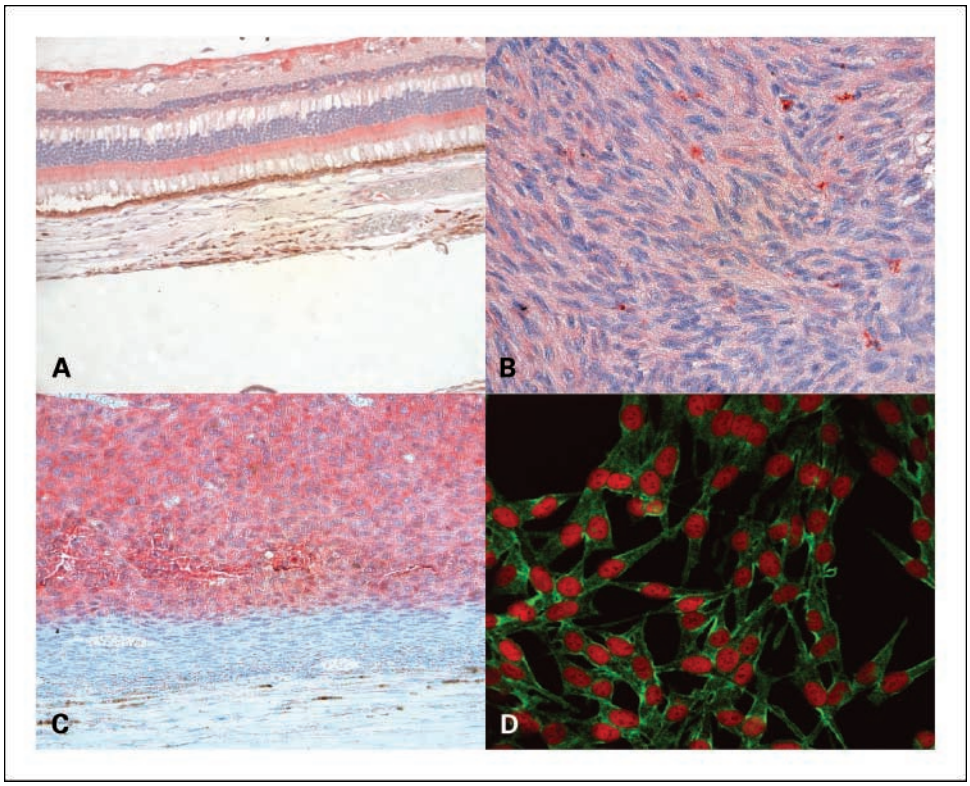

Fig. 1. *A,* Hsp90 staining of retinal tissue in ganglion cell layer and inner and outer plexiform layer and low percentage of Hsp90 staining in the choroids. Original magnification, ×200. *B,* spindle cell uveal melanoma stained for Hsp90 showing medium staining intensity. Original magnification, ×400. *C,* epithelioid cell uveal melanoma stained for Hsp90. In comparison with the tumor, the spindle A (nevus) at the base of the tumor and also the choroid display low percentage of Hsp90 staining. Original magnification, ×400. *D,* green, expression of Hsp90α in uveal melanoma cell line visualized by confocal microscopy showing membranous staining. Original magnification, ×400.

melanoma cells and cells treated with 10 μmol/L/mL 17-AAG for 24 h were resuspended in 1 mL of RPMI 1640 at a concentration of 1×10^6/mL. Samples were incubated on ice for 30 min, washed with PBS, and resuspended in cold staining buffer containing 0.1% sodium citrate, 0.2 mg/mL RNase, 0.3% NP40, and 50 g/mL propidium iodide. After labeling with propidium iodide, the cells were analyzed for DNA cycle using an Epics XL flow cytometer (Beckman Coulter). The percentage of cells in G_1, the S-phase fraction, and G_2 was recorded along with cellular DNA ploidy.

Caspase-3 protease activity assay. The caspase-3 protease activity was detected using the BD ApoAlert Caspase Colorimetric Assay (BD Biosciences Clontech) according to the manufacturer's protocol. Briefly, following a 48-h incubation with and without 17-AAG (10 μmol/L), 1×10^6 cells/mL were counted, centrifuged, and resuspended in cell lysis buffer. The cell lysates were centrifuged for 10 min and supernatant samples of 50 μL from each cell line and controls were allowed to react with 50 μL of 2× reaction buffer/DTT mix and 1 μL of caspase-3 inhibitor followed by 30-min incubation on ice. Caspase-3 substrate was then added to each reaction and the cells were incubated at 37°C for 1 h. The samples were read in a microplate reader using a spectrophotometer at 405 nm. The experiments were repeated in triplicate.

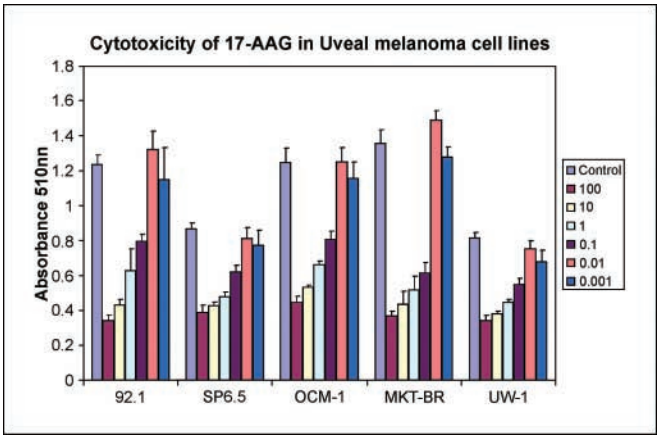

Fig. 2. SulforhodamineTOX-6 assay showing the effect of 17-AAG on proliferation of the five uveal melanoma cell lines compared with control at a concentration ranging from 100 to 0.001 μmol/L. Significant inhibition ($P < 0.001$) of cellular proliferation was seen at concentrations ranging from 0.1 to 100 μmol/L.

Apoptosis assay. Apoptosis was determined by terminal deoxynucleotidyl transferase–mediated dUTP nick end labeling assay by flow cytometry using 10 μmol/L 17-AAG (Apo-Direct, BD Biosciences) according to the instructions of the manufacturer. Briefly, cells were harvested, washed in PBS, fixed with 70% ethanol, and incubated with FITC-dUTP for 60 min at 37°C. Data were collected and analyzed with Epics XL flow cytometer using CellQuest Pro software (BD Biosciences).

Western blot analysis. Cell lines were incubated with and without 10 μmol/L 17-AAG for 24, 48, and 72 h. Cells were lysed on ice in TNESV (50 mmol/L Tris-HCl, 1% NP40, 2 mmol/L EDTA, 100 mmol/L NaCl, 1 mmol/L orthovanadate) containing protease inhibitor cocktail (Sigma-Aldrich) and the lysate was cleared by centrifugation for 10 min at 12,000 × *g*. Protein determination was made using Bio-Rad protein assay (Bio-Rad Laboratories). Protein aliquots of 10 μg were loaded onto 10% to 12% SDS-PAGE gel and then transferred to polyvinylidene difluoride (Millipore) membrane.

The membrane was blotted for the specific antibodies monoclonal mouse anti-Hsp90 and anti-Hsp70 (StressGen), polyclonal rabbit anti-Akt and polyclonal rabbit anti-phosphorylated Akt (p-Akt; Ser^{473}; Cell Signaling Technology), and monoclonal anti-CDK4 and anti-cyclin D1 (Cell Signaling Technology). Immunoblotting with anti-actin antibodies was done to confirm equal protein loading (Santa Cruz Biotechnology). Further, horseradish peroxidase–conjugated goat anti-mouse or goat anti-rabbit secondary antibody (Santa Cruz Biotechnology) was applied. Detection was done using enhanced chemiluminescence with autoradiographic film (Hyperfilm ECL, GE Healthcare).

Statistical analysis. Statistical analyses for patient samples were done using computer-based statistical package (MedCalc Statistical Package, version 9.2.0.2, Mariakerke). Separate analyses were made for each of the patient groups. The association between Hsp90 expression and age at diagnosis, sex, cell type, and LTD was determined using the correlation coefficient test. The association between Hsp90 expression and the incidence of metastasis was assessed using the Kaplan-Meier survival analysis and log-rank test. The Student's t test and χ^2 analysis were used where appropriate for the *in vitro* studies. A P value of <0.05 was considered statistically significant.

Results

Immunohistochemistry. Forty-four cases of uveal melanoma were studied. Twenty-eight patients were males and the age of the patients ranged from 32 to 82 years (mean, 61). Seventy-seven percent of tumors (n = 34) were classified as mixed cell type, 4.5% (n = 2) as epithelioid cell type, and 18.8% (n = 8) as spindle cell type.

Overall, 68% of cases (n = 30) were Hsp90 positive. Hsp90 was also expressed in the retinal pigment epithelium, both the inner and outer plexiform retinal layers, and the ganglion cell layer. The normal choroidal melanocytes displayed a low degree of staining. In addition, in four cases, we were able to determine that, in comparison with the tumor, the spindle A cells (nevus) at the base of the tumor presented low Hsp90 staining. In tumor cells, immunoreactivity specific to Hsp90 was detected both in the cytoplasm and in the nuclei of the positive cells (Fig. 1).

Fifty percent of the tumors (22 of 44) had a high score of Hsp90 immunostaining with >50% cells stained and a moderate to high degree of staining intensity. Hsp90 stained positive in 61.5% (n = 16) of the 26 patients in the primary enucleation group and 50% (n = 13) of those cases were classified as high Hsp90 expression. In the group of patients treated with radiotherapy before enucleation (n = 16), Hsp90 stained positive in 68% (n = 11) of cases and high expression was seen in 43.75% (n = 7). Two patients (4.5%) underwent transscleral thermotherapy before enucleation and both had a high degree of Hsp90 immunostaining.

The mean LTD was 13.54 mm. In the positive Hsp90 group, the mean LTD was 14.10 mm, whereas in the high Hsp90 expression group the mean LTD was 14.69 mm. In the negative

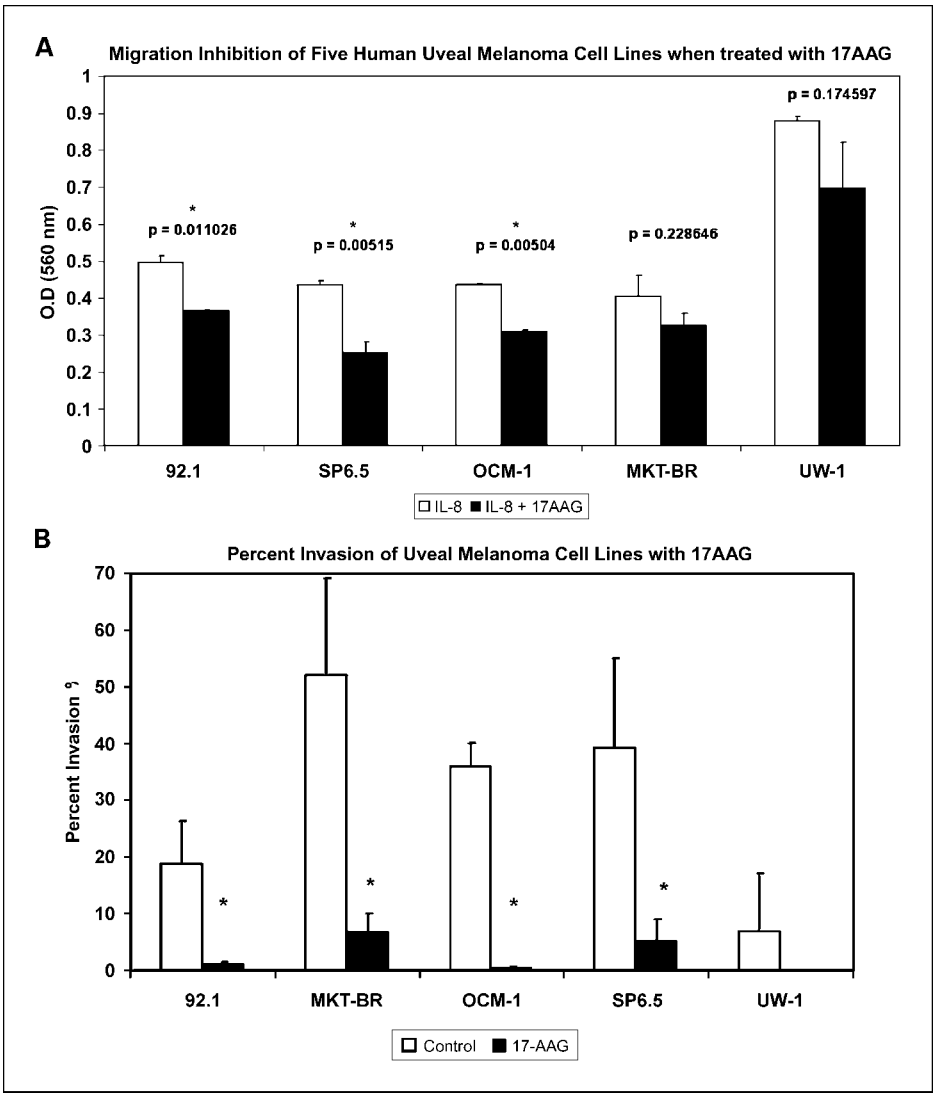

Fig. 3. *A,* motility assay showing a reduction in the migratory capacity of the uveal melanoma cells on addition of 17-AAG with statistical significance in three of the most invasive cell lines (92.1, SP6.5, and OCM-1). *B,* percentage of invasion of uveal melanoma cells with and without addition of 17-AAG showing a significant reduction in invasion ability of all cell lines. Columns, mean of three experiments; bars, SE.

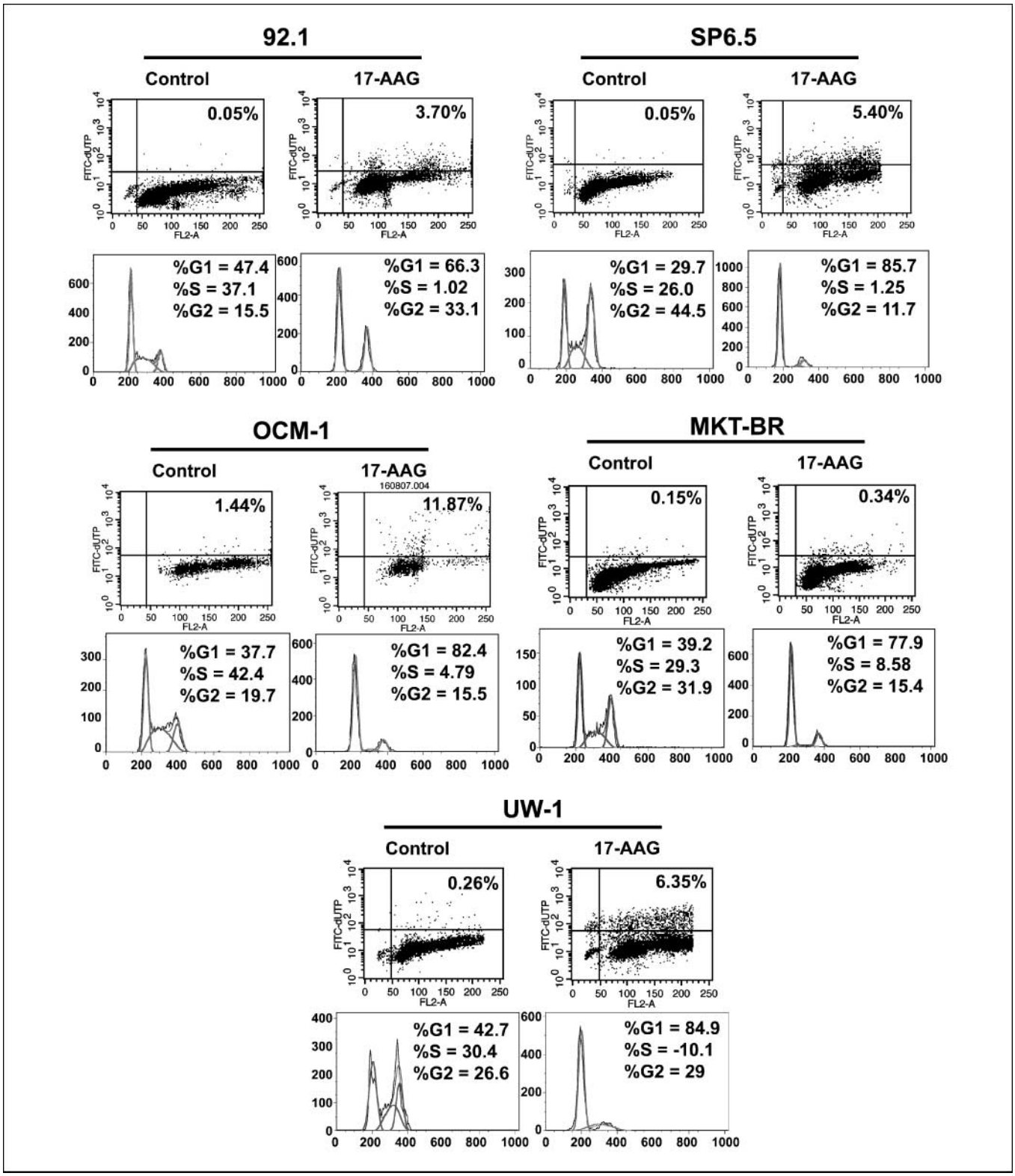

Fig. 4. Top, in uveal melanoma cells, 17-AAG induced apoptosis (cells positive for FITC-dUTP) after 48 h compared with control cells; bottom, cell cycle fractions of the uveal melanoma cells with and without 17-AAG showing that the drug induces G_0-G_1 cell cycle arrest. *X* axis, FL2-H:propidium iodide; *Y* axis, number of cells.

staining group, the mean LTD was 12.1 mm. There was a significant correlation between high expression of Hsp90 and a larger LTD (P = 0.03). No correlation was found between intensity and percentage of Hsp90 and cell type or previous radiotherapy treatment (P > 0.05). At the end of the follow-up period (average, 83 months), 45.4% (n = 20) of patients developed metastasis. Although in this group there was a difference between Hsp90-positive (75%; n = 15) and

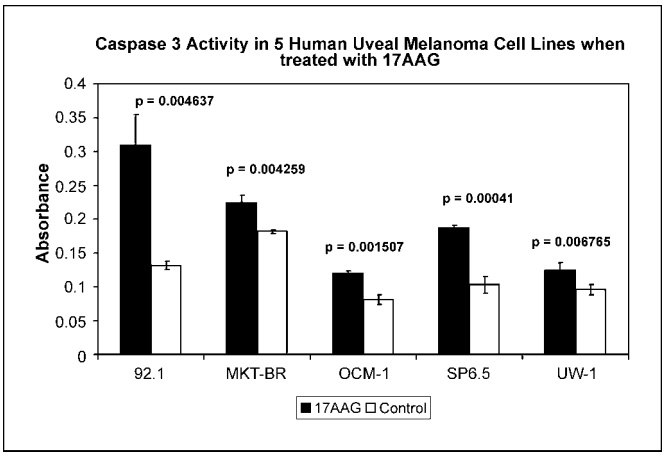

Fig. 5. Caspase-3 protease activity assay showing an increase in caspase-3 on exposure of uveal melanoma cell lines (92.1, OCM-1, SP6.5, MKT-BR, and UW-1) to 17-AAG. Columns, mean of three experiments; bars, SE.

Hsp90-negative tumors (25%; $n = 5$), Kaplan-Meier test showed that intensity and distribution of staining was not related to survival rate ($P > 0.05$).

Immunocytochemistry. Cytospins of each uveal melanoma cell line were positive for Hsp90 staining. Hsp90 was mostly intracytoplasmatically expressed in all cell lines tested, with a subpopulation of these positive cells showing concomitant membranous and nuclear Hsp90 expression. The degree of staining was similar in each of the five cell lines (92.1, SP6.5, MKT-BR, OCM-1, and UW-1). Immunofluorescence detected expression of Hsp90α on the cell membrane of all five cell lines (Fig. 1).

Proliferation assay. Significant inhibition ($P < 0.001$) of cellular proliferation was seen in all uveal melanoma cell lines after exposure to 17-AAG compared with controls at concentrations ranging from 0.1 to 100 μmol/L (Fig. 2). From the dose-response data, corrected for the cell count at time zero, we calculated the percentages of growth inhibition at different drug concentrations using the formula: $GI = 100 \times (T - T_0) / (C - T_0)$. GI_{50} values were determined by nonlinear regression analysis for a dose-response curve, using the equation for a sigmoid plot, using GraphPad Prism version 3 (20).

Growth-inhibitory concentration, GI_{50} values, ranged from 50 to 137 nmol/L (average, 109 nmol/L). The corresponding GI_{50} values (mean ± SD) were 123 ± 0.33, 142 ± 0.17, 93 ± 0.27, 50 ± 0.37, and 137 ± 0.3 for 92.1, SP6.5, MKT-BR, OCM-1 and UW-1, respectively. In the subsequent experiments, the concentration of 17-AAG that significantly inhibited the proliferation of the uveal melanoma cell lines (the submaximal concentration of 10 μmol/L) was chosen to obtain a maximum effect of Hsp90 inhibition. In addition, pharmacokinetic analysis from patient phase I clinical trials indicated that, at the highest drug dose, plasma 17-AAG concentrations achieved or exceeded 10 μmol/L (9, 20).

Migration assay. All five human uveal melanoma cell lines migrated toward the selected chemoattractant CXCL8 at a level greater than the selected negative control (serum-free RPMI 1640). The migratory capacity of the uveal melanoma cells was significantly reduced in three of the cell lines (92.1, SP6.5, and OCM-1) on addition of 17-AAG (10 μmol/L; Fig. 3A).

Invasion assay. The average number of cells that invaded the Matrigel baseline decreased significantly after addition of 17-AAG from 7 ± 3.6 to 0.4 ± 0.6 ($P = 1.64E^{-07}$) for 92.1, from 6.9 ± 6.5 to 0.8 ± 1.2 ($P = 0.001$) for SP6.5, from 38.6 ± 17.6 to 0.66 ± 0.89 ($P = 4.61E^{-09}$) for OCM-1, from 9.7 ± 5.4 to 1.33 ± 1.44 ($P = 3.72E^{-06}$) for MKT-BR, and from 7.33 ± 9.68 to 0 ± 0 ($P = 0.006$) for UW-1. The average results of percentage invasion from three experiments were at baseline: MKT-BR, 52.10 ± 17.04; SP6.5, 39.21 ± 15.92; OCM-1, 35.8 ± 4.20; 92.1, 18.74 ± 7.69; and UW-1, 6.92 ± 10.13. The addition of 17-AAG decreased the percentage invasion in all cell lines: MKT-BR, 6.89 ± 3.14; SP6.5, 5.37 ± 3.76; 92.1, 1.23 ± 0.26; OCM-1, 0.62 ± 0.11; and UW-1, 0 ± 0 (Fig. 3B).

Cell cycle analysis. Treatment of the five (92.1, SP6.5, MKT-BR, OCM-1, and UW-1) cell lines with 10 μmol/L 17-AAG for 24 h induced an increase in percentage of cells in the G_1 compared with baseline of 15.24% for 92.1, 54.3% for SP6.5, 42.44% for OCM-1, 36.82% for UW-1, and 37.95% for MKT-BR (Fig. 4).

Apoptosis terminal deoxynucleotidyl transferase–mediated dUTP nick end labeling assay. In uveal melanoma cells, 17-AAG induced cell death (cells positive for FITC-dUTP) after 48 h compared with control cells. FITC-dUTP–positive cells were 3.70%, 5.40%, 11.87%, 0.34%, and 6.35% in 17-AAG–treated 92.1, SP6.5, OCM-1, MKT-BR, and UW-1, whereas control cells showed 0.05%, 0.05%, 1.44%, 0.15%, and 0.26% cell death, respectively (Fig. 4).

Caspase-3 protease activity assay. Treatment of the five cell lines with 10 μmol/L 17-AAG for 48 h showed significantly higher levels of activated caspase-3 from 0.124 ± 0.006 to 0.277 ± 0.04 for 92.1, from 0.107 ± 0.01 to 0.190 ± 0.004 for SP6.5, from 0.084 ± 0.006 to 0.120 ± 0.003 for OCM-1, from 0.182 ± 0.002 to 0.218 ± 0.010 for MKT-BR, and from 0.089 ± 0.007 to 0.129 ± 0.010 for UW-1, indicating a execution of the mitochondrial/intrinsic apoptosis pathway. The histogram figure represents average results from three separate experiments (Fig. 5).

Western blotting. Immunoblotting was used to examine the ability of a Hsp90 inhibitor to influence the expression of Hsp90 and cochaperone Hsp70, CDK4, cyclin D1, Akt, and p-Akt. In all five cell lines, Hsp70 was up-regulated after 24 h of exposure to 17-AAG, and also a slight increase in Hsp90 expression was seen, indicating a stress response to Hsp90 inhibition. In all the lines, a decrease in Akt and a marked decrease in levels of p-Akt were seen.

Treatment of uveal melanoma cells with 17-AAG predominantly induced G_1 cell cycle arrest, which was associated with down-regulation of CDK4. Expression of cyclin D1 was modestly down-regulated by 17-AAG in SP6.5 cells and remained unchanged in 92.1, OCM-1, MKT-BR, and UW-1. The results of Western blot analysis are presented in Fig. 6.

Discussion

Hsp90 has previously been shown to be expressed in higher levels in tumors, forming large complexes with other chaperones and "client proteins" (21). Hsp90 expression and its therapeutic implications depend on the tumor type. Increased expression of Hsp90 was observed in cutaneous melanoma, breast tumors, lung cancer, leukemias, and Hodgkin's disease (5, 13, 22, 23) and has been shown to correlate with an

increase in malignant phenotype in breast cancer (24) and gastric cancer (25). Conversely, the expression of Hsp90 is associated with good prognosis in endometrial cancer (26), whereas expression of Hsp90 was seen to be of no prognostic significance in ovarian cancer (27) and salivary gland tumors (28).

In uveal melanoma, a single previous study has reported expression of Hsp90, which was found to be expressed in 60% of cases; however, the average percentage of tumor cell staining reported was of 6% (29). In comparison with previous results, we showed a higher degree of positive staining in our uveal melanoma cases, with 68% of cases staining positive and an average of 50% of tumor cells stained. This high expression of Hsp90 was positively correlated with largest tumor diameter, a clinical indicator of worse prognosis (30). This difference in expression, compared with the prior study, may be related to differences in immunohistochemical methods, including different detection methods, case selection, and possible differences in embedding and processing techniques. Our results indicate that Hsp90 in uveal melanoma is a promising potential therapeutic target. Although the expression of Hsp90 may increase after radiotherapy stress, we found no difference in staining between those patients treated by enucleation only versus radiotherapy followed by enucleation.

The monoclonal antibody used in the current study allowed the detection of both isoforms of Hsp90 (α and β) and its expression was shown to be predominantly intracytoplasmatic. We also showed that Hsp90α was present on the surface of our uveal melanoma cells *in vitro*, suggesting possible extracellular roles for Hsp90 (31). Recently, functional proteomic analysis correlated extracellular expression of Hsp90α with increased cancer cell invasiveness (32).

Different mechanisms have been described as contributing to the molecular pathogenesis of uveal melanoma, including mutations in p53, overexpression of Bcl-2, cyclin D1, and c-myc (33, 34). Different tumor cell models have shown that the c-myc proto-oncogene directly activates Hsp90 transcription (35), and it has been reported that this chaperone stabilizes the conformations of mutant proteins that arise during transformation, such as p53 (36). It is tempting to speculate that overexpression of Hsp90 may play a role in uveal melanoma through interaction of Hsp90 with several client proteins involved in cell proliferation and survival. Hsp90 was not found to be an independent indicator of poor prognosis in our patient samples, which might be due to either the size of our sample or the follow-up data. However, our data showed that high expression of Hsp90 was associated with the largest tumor diameter, which is the most significant clinical prognostic indicator for high risk of metastasis in uveal melanoma. This suggests that the evaluation of Hsp90 expression in uveal melanoma could predict aggressive behavior of these tumor cells. Therefore, the wide expression of Hsp90 makes it a possible therapeutic target in uveal melanoma in the future.

As previously mentioned, no prior study investigated the role of Hsp90 and the effects of its inhibition in uveal melanoma. We have shown that the Hsp90 inhibitor 17-AAG caused a marked reduction in the proliferation of uveal melanoma cell lines of different metastatic and invasive potential. 17-AAG

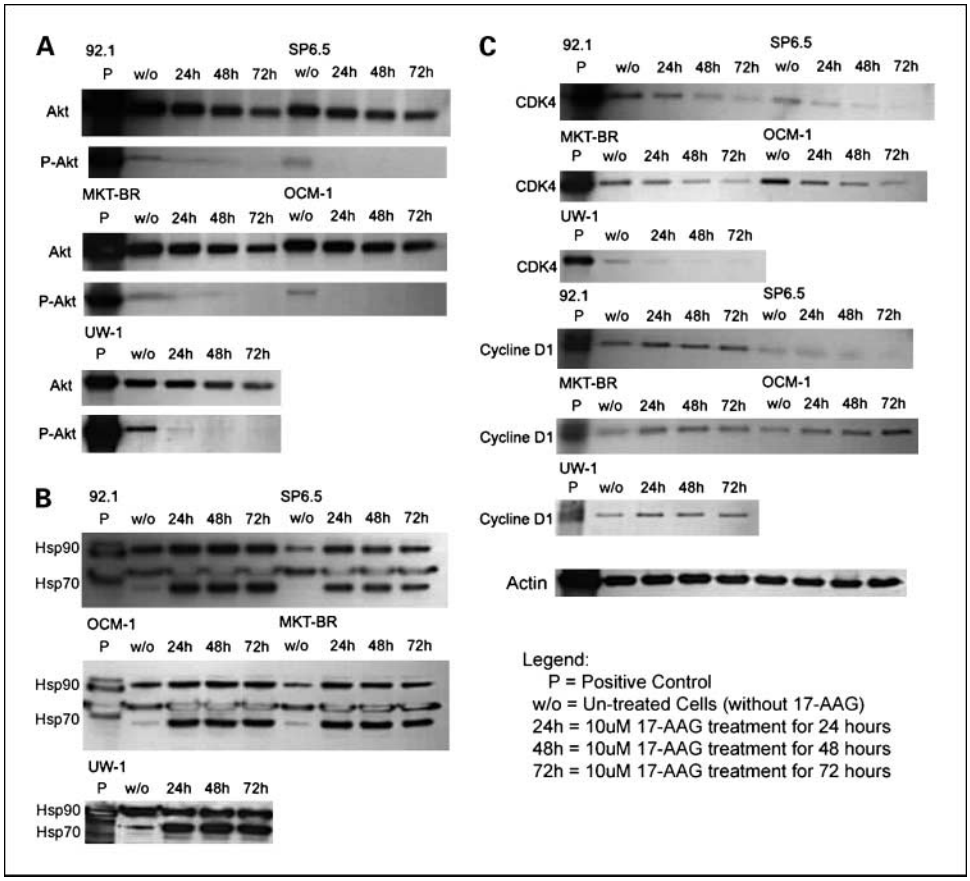

Fig. 6. *A,* 17-AAG down-regulated the expression of Akt and p-Akt levels starting with 24 h of exposure. *B,* 17-AAG up-regulated the expression of Hsp70 at 24 h of exposure and also a slight up-regulation of Hsp90 levels was seen. *C,* 17-AAG down-regulated the expression of CDK4 levels starting with 24 h of exposure. P, positive control; w/o, without 17-AAG exposure.

exhibited a differential cytotoxicity profile against different cell lines, with an average growth-inhibitory concentration (GI_{50}) over all cell lines of 109 nmol/L, comparable with the cutaneous melanoma subpanel (37). Two of the cell lines with the most aggressive, invasive, and metastatic phenotype (92.1 and SP6.5) were relatively less sensitive to the agent (123 and 143 nmol/L, respectively). However, the exposure to 17-AAG at doses comparable with peak plasma concentrations achieved in phase I clinical trials (9, 20) significantly decreased the migratory and invasive ability of all human uveal melanoma cell lines, including the most aggressive ones. Although Hsp90 had a different basal expression, the drug affected all cell lines, and there was no correlation between basal level of Hsp90 and drug response. These results are in accordance with previous studies in breast cancer cell lines, where such correlation also could not be found (24). The association between Hsp90 expression and the response to Hsp90 inhibitors is not fully elucidated, but possibly the response could be dictated by the activity of the Hsp90 and the depletion of a specific oncogenic protein implicated in tumor progression.

Inhibition of Hsp90 by 17-AAG caused an increase in Hsp90 and Hsp70 proteins as measured by Western blot indicating a stress response, a sensitive pharmacodynamic end point used to monitor the drug activity (20). Our results are similar with the results obtained in other cancers indicating an increase in Hsp90 after drug inhibition (e.g., in Hodgkin's lymphoma cells; ref. 38).

One possible effect of Hsp90 inhibition is dysregulation of the Akt pathway, which can result in reduction in signal transduction, proliferation, and invasion (39). p-Akt has been previously shown to be associated with a higher risk of metastatic disease in uveal melanoma (40), and recent studies have shown that Akt relies on Hsp90 for its stability (41). In our study, the exposure of our human uveal melanoma cell lines to 17-AAG resulted in a decrease of Akt and activated p-Akt, possibly contributing to induction of cell growth arrest and death.

Other mechanisms leading to survival and progression in uveal melanoma occur in the presence of inappropriate mitogenic stimuli, through inactivation of the retinoblastoma protein by hyperphosphorylation, possibly due to the overexpression of cyclin D1 (34) and activation of endogenous CDK4 and CDK6 (42). Cell cycle analysis in this study showed that exposure to 17-AAG resulted in a G_1 cell cycle arrest in all of the human uveal melanoma cell lines, associated with decline in the levels of cell regulatory protein CDK4. Cyclin D1 was moderately reduced in SP6.5 cell line possibly due to down-regulation of the phosphatidylinositol 3-kinase-Akt–dependent pathway that is required for its expression (43). However, although Akt and p-Akt were down-regulated, expression of cyclin D1 remained unchanged in the other four uveal melanoma cell lines, suggesting a different mechanism of regulation. The mechanisms behind the G_1 cell cycle arrest remain to be understood in detail but previous studies have shown that the maturation of CDK4 is dependent on Hsp90 and this kinase was shown to be a direct target of the drug (44). Our results suggest that 17-AAG selectively inhibited pathways required for cyclin D1–associated CDK4 activity (38).

The reduced efficacy of many chemotherapeutic drugs in uveal melanoma is due to their relative inability to induce apoptosis. Furthermore, resistance to apoptosis has been correlated with an increase in the metastatic potential of uveal melanoma in animal models (45). Similar to other studies (38, 46), inhibition of signal transduction by agents such as 17-AAG resulted in cell apoptosis. The expression of Hsp90 has been implicated in the regulation of apoptosis by binding APAF-1 and Bcl-2 (47) and also by its capacity to interact with p-Akt (48). Because the activity and stability of Akt is dependent on Hsp90 in tumor cells, down-regulation of Akt expression with 17-AAG may render uveal melanoma cells susceptible to induced apoptosis. Inhibition of Hsp90 may also promote apoptosis in uveal melanoma through other mechanisms that remain to be examined. The effect of 17-AAG on caspase-3 expression in uveal melanoma has not previously been reported. Our results showed an increase in the apoptotic marker caspase-3 after 17-AAG administration in all uveal melanoma cell lines, indicating execution of the mitochondrial intrinsic pathway, therefore modifying that the apoptotic program in uveal melanoma cells through inhibition of Hsp90 may be a useful strategy for overcoming drug resistance. Targeting Hsp90 may also prove to be beneficial as an adjuvant therapy coupled with traditional therapeutics. Due to the inhibition of survival signaling through the degradation of proteins such as Akt, or through induction of cell cycle arrest, this therapy may render uveal melanoma cells more susceptible to chemotherapy.

Because normal cells also express Hsp90, it is a concern whether its inhibition would affect nonneoplastic tissues, limiting the applicability of this therapeutic approach. In a previous study for tumor selectivity of Hsp90 inhibitor, it was shown that Hsp90 in normal cells exists in an uncomplexed form that has low affinity for Hsp90 inhibitor drugs. Conversely, Hsp90 in cancer cells exists in a complexed form with cochaperone proteins and exhibits high-affinity binding to Hsp90 inhibitor drugs (21). Therefore, we believe that a differential effect can be achieved with a Hsp90 inhibitor in uveal melanoma cells versus normal cells.

In conclusion, we have shown for the first time in uveal melanoma that the high expression of Hsp90 correlates with a marker of poor prognosis and also is involved in proliferation, migration, and invasion processes. Inhibition of Hsp90 by 17-AAG can modulate all these processes and also resulted in the destabilization of p-Akt leading to proapoptotic and antiproliferative effects. Searching for new molecular therapeutic targets in uveal melanoma is of great importance and modulation of multiple signaling pathways through inhibition of Hsp90 may represent a new therapeutic modality in uveal melanoma.

References

1. Egan KM, Seddon JM, Glynn RJ, Gragoudas ES, Albert DM. Epidemiologic aspects of uveal melanoma. Surv Ophthalmol 1988;32:239–51.
2. Bedikian AY. Metastatic uveal melanoma therapy: current options. Int Ophthalmol Clin 2006;46:151–66.
3. Maloney A, Workman P. HSP90 as a new therapeutic target for cancer therapy: the story unfolds. Expert Opin Biol Ther 2002;2:3–24.
4. Buchner J. Hsp90 & Co.—a holding for folding. Trends Biochem Sci 1999;24:136–41.
5. Whitesell L, Lindquist SL. HSP90 and the chaperoning of cancer. Nat Rev Cancer 2005;5:761–72.
6. Burrows F, Zhang H, Kamal A. Hsp90 activation and cell cycle regulation. Cell Cycle 2004;3:1530–6.
7. Niikura Y, Ohta S, Vandenbeldt KJ, Abdulle R, McEwen BF, Kitagawa K. 17-AAG, an Hsp90 inhibitor, causes kinetochore defects: a novel mechanism by

which 17-AAG inhibits cell proliferation. Oncogene 2006;25:4133–46.

8. Solit DB, Ivy SP, Kopil C, et al. Phase I trial of 17-allylamino-17-demethoxygeldanamycin in patients with advanced cancer. Clin Cancer Res 2007;13:1775–82.

9. Nowakowski GS, McCollum AK, Ames MM, et al. A phase I trial of twice-weekly 17-allylamino-demethoxy-geldanamycin in patients with advanced cancer. Clin Cancer Res 2006;12:6087–93.

10. Marshall JC, Caissie AL, Callejo SA, Antecka E, Burnier MN, Jr. Cell proliferation profile of five human uveal melanoma cell lines of different metastatic potential. Pathobiology 2004;71:241–5.

11. McLean IW, Foster WD, Zimmerman LE, Gamel JW. Modifications of Callender's classification of uveal melanoma at the Armed Forces Institute of Pathology. Am J Ophthalmol 1983;96:502–9.

12. McLean IW, Foster WD, Zimmerman LE. Uveal melanoma: location, size, cell type, and enucleation as risk factors in metastasis. Hum Pathol 1982;13:123–32.

13. Becker B, Multhoff G, Farkas B, et al. Induction of Hsp90 protein expression in malignant melanomas and melanoma metastases. Exp Dermatol 2004;13:27–32.

14. Detre S, Saclani Jotti G, Dowsett M. A "quickscore" method for immunohistochemical semiquantitation: validation for oestrogen receptor in breast carcinomas. J Clin Pathol 1995;48:876–8.

15. Cappello F, David S, Ardizzone N, et al. Expression of heat shock proteins hsp10, hsp27, hsp60, hsp70, and hsp90 in urothelial carcinoma of urinary bladder. J Can Mol 2006;2:73–7.

16. De Waard-Siebinga I, Blom DJ, Griffioen M, et al. Establishment and characterization of an uveal-melanoma cell line. Int J Cancer 1995;62:155–61.

17. Albert DM, Ruzzo MA, McLaughlin MA, Robinson NL, Craft JL, Epstein J. Establishment of cell lines of uveal melanoma. Methodology and characteristics. Invest Ophthalmol Vis Sci 1984;25:1284–99.

18. Di Cesare S, Marshall JC, Logan P, et al. Expression and migratory analysis of 5 human uveal melanoma cell lines for CXCL12, CXCL8, CXCL1, and HGF. J Carcinog 2007;6:2.

19. Woodward JK, Elshaw SR, Murray AK, et al. Stimulation and inhibition of uveal melanoma invasion by HGF, GRO, IL-1α and TGF-β. Invest Ophthalmol Vis Sci 2002;43:3144–52.

20. Banerji U, O'Donnell A, Scurr M, et al. Phase I pharmacokinetic and pharmacodynamic study of 17-allylamino, 17-demethoxygeldanamycin in patients with advanced malignancies. J Clin Oncol 2005;23:4152–61.

21. Kamal A, Thao L, Sensintaffar J, et al. A high-affinity conformation of Hsp90 confers tumour selectivity on Hsp90 inhibitors. Nature 2003;425:407–10.

22. Hsu PL, Hsu SM. Abundance of heat shock proteins (hsp89, hsp60, and hsp27) in malignant cells of Hodgkin's disease. Cancer Res 1998;58:5507–13.

23. Yano M, Naito Z, Tanaka S, Asano G. Expression and roles of heat shock proteins in human breast cancer. Jpn J Cancer Res 1996;87:908–15.

24. Pick E, Kluger Y, Giltnane JM, et al. High HSP90 expression is associated with decreased survival in breast cancer. Cancer Res 2007;67:2932–7.

25. Zuo DS, Dai J, Bo AH, Fan J, Xiao XY. Significance of expression of heat shock protein90α in human gastric cancer. World J Gastroenterol 2003;9:2616–8.

26. Nanbu K, Konishi I, Mandai M, et al. Prognostic significance of heat shock proteins HSP70 and HSP90 in endometrial carcinomas. Cancer Detect Prev 1998;22:549–55.

27. Elpek GO, Karaveli S, Simsek T, Keles N, Aksoy NH. Expression of heat-shock proteins hsp27, hsp70 and hsp90 in malignant epithelial tumour of the ovaries. APMIS 2003;111:523–30.

28. Vanmuylder N, Evrard L, Daelemans P, Van Reck J, Dourov N. [Expression of heat shock proteins in salivary gland tumors. Immunohistochemical study of HSP27, HSP70, HSP90, and HSP110: apropos of 50 cases]. Ann Pathol 2000;20:190–5.

29. Missotten GS, Journee-de Korver JG, de Wolff-Rouendaal D, Keunen JE, Schlingemann RO, Jager MJ. Heat shock protein expression in the eye and in uveal melanoma. Invest Ophthalmol Vis Sci 2003;44:3059–65.

30. McLean IW, Saraiva VS, Burnier MN Jr. Pathological and prognostic features of uveal melanomas. Can J Ophthalmol 2004;39:343–50.

31. Schmitt E, Gehrmann M, Brunet M, Multhoff G, Garrido C. Intracellular and extracellular functions of heat shock proteins: repercussions in cancer therapy. J Leukoc Biol 2007;81:15–27.

32. Eustace BK, Jay DG. Extracellular roles for the molecular chaperone, hsp90. Cell Cycle 2004;3:1098–100.

33. Ehlers JP, Harbour JW. Molecular pathobiology of uveal melanoma. Int Ophthalmol Clin 2006;46:167–80.

34. Coupland SE, Bechrakis N, Schuler A, et al. Expression patterns of cyclin D1 and related proteins regulating G_1-S phase transition in uveal melanoma and retinoblastoma. Br J Ophthalmol 1998;82:961–70.

35. Teng SC, Chen YY, Su YN, et al. Direct activation of HSP90A transcription by c-Myc contributes to c-Myc-induced transformation. J Biol Chem 2004;279:14649–55.

36. Neckers L, Lee YS. Cancer: the rules of attraction. Nature 2003;425:357–9.

37. Burger AM, Fiebig HH, Stinson SF, Sausville EA. 17-(Allylamino)-17-demethoxygeldanamycin activity in human melanoma models. Anticancer Drugs 2004;15:377–87.

38. Georgakis GV, Li Y, Rassidakis GZ, Martinez-Valdez H, Medeiros LJ, Younes A. Inhibition of heat shock protein 90 function by 17-allylamino-17-demethoxygeldanamycin in Hodgkin's lymphoma cells down-regulates Akt kinase, dephosphorylates extracellular signal-regulated kinase, and induces cell cycle arrest and cell death. Clin Cancer Res 2006;12:584–90.

39. Vivanco I, Sawyers CL. The phosphatidylinositol 3-kinase AKT pathway in human cancer. Nat Rev Cancer 2002;2:489–501.

40. Saraiva VS, Caissie AL, Segal L, Edelstein C, Burnier MN, Jr. Immunohistochemical expression of phospho-Akt in uveal melanoma. Melanoma Res 2005;15:245–50.

41. Fujiwara H, Yamakuni T, Ueno M, et al. IC101 induces apoptosis by Akt dephosphorylation via an inhibition of heat shock protein 90-ATP binding activity accompanied by preventing the interaction with Akt in L1210 cells. J Pharmacol Exp Ther 2004;310:1288–95.

42. Sherr CJ. Cancer cell cycles. Science 1996;274:1672–7.

43. Muise-Helmericks RC, Grimes HL, Bellacosa A, Malstrom SE, Tsichlis PN, Rosen N. Cyclin D expression is controlled post-transcriptionally via a phosphatidylinositol 3-kinase/Akt-dependent pathway. J Biol Chem 1998;273:29864–72.

44. Stepanova L, Leng X, Parker SB, Harper JW. Mammalian p50Cdc37 is a protein kinase-targeting subunit of Hsp90 that binds and stabilizes Cdk4. Genes Dev 1996;10:1491–502.

45. Li H, Niederkorn JY, Neelam S, Alizadeh H. Resistance and susceptibility of human uveal melanoma cells to TRAIL-induced apoptosis. Arch Ophthalmol 2005;123:654–61.

46. Hostein I, Robertson D, DiStefano F, Workman P, Clarke PA. Inhibition of signal transduction by the Hsp90 inhibitor 17-allylamino-17-demethoxygeldanamycin results in cytostasis and apoptosis. Cancer Res 2001;61:4003–9.

47. Pandey P, Saleh A, Nakazawa A, et al. Negative regulation of cytochrome *c*-mediated oligomerization of Apaf-1 and activation of procaspase-9 by heat shock protein 90. EMBO J 2000;19:4310–22.

48. Solit DB, Basso AD, Olshen AB, Scher HI, Rosen N. Inhibition of heat shock protein 90 function down-regulates Akt kinase and sensitizes tumors to Taxol. Cancer Res 2003;63:2139–44.